**Available Online at www.ijcsmc.com**

**International Journal of Computer Science and Mobile Computing**

**A Monthly Journal of Computer Science and Information Technology**

**ISSN 2320–088X**
**IMPACT FACTOR: 7.056**

***IJCSMC, Vol. 15, Issue. 2, February 2026, pg.62 – 71***

# Land Use-Cover Change Modelling Using Deep Learning Techniques with a focusing on an Agrarian Community

**Johnson O.E[1]; Ganiyu M.[2]; Enigbokan O. Y.[3]; Adekunle K. O[4]**

[1,2,3,4]Department of Computer Science, Federal Polytechnic, Ile-Oluji, Ondo State, Nigeria
[1] estjohnson@fedpolel.edu.ng

**DOI: https://doi.org/10.47760/ijcsmc.2026.v15i02.007**

**Abstract: Land use change detection modelling is critical to understanding the dynamics of natural and human-induced environmental transformations. It embodies profound implications for agricultural productivity, food security, and sustainable land management, particularly in developing agrarian communities. While existing studies provide some insight, it is important to investigate modern techniques for further improvement. This study, therefore, proposes a Convolutional Neural Network (CNN)-Channel-wise Attention (CNN-CwA) deep learning model for land-use and land-cover change (LULCC) classification. It integrates a CwA mechanism into a CNN backbone to enable dynamic spectral channel recalibration and improve land cover discrimination in heterogeneous agrarian landscapes. The model is trained and validated on the EuroSAT benchmark dataset, comprising 27,000 geo-referenced Sentinel-2 satellite image patches spanning ten land cover classes. A five-fold cross-validation strategy was employed alongside t-Distributed Stochastic Neighbour Embedding (t-SNE) visualisation to assess model generalisation and feature discriminability. The CNN-CwA model achieved a mean Intersection over Union (mIoU) of 0.8852, representing a 2.86% improvement over the baseline CNN (mIoU = 0.8606), with notable per-class gains for Sea or Lake of +0.0811, Pasture of +0.0365, River of +0.0292, and Highway of +0.0288. Vegetation-related classes including Forest, Herbaceous Vegetation, and Permanent Crop all exceeded the 0.90 IoU threshold. The findings affirm the model's reliability for agronomically relevant land cover discrimination. In addition, it demonstrates the practical utility of the CNN-CwA model as a robust and scalable tool for LULCC classification in agrarian landscapes. The model also serves as a computational foundation for evidence-based agricultural land use planning and food security policy formulation in Nigeria and similar developing-country contexts.**

**Keywords: Land-use, Change Modeling, Convolutional Neural Network, Channel-wise attention, Remote sensing**

 

## I. INTRODUCTION

Land use change detection is helping to determine how land use and land cover patterns shift over time. It offers critical insights into the interplay between human activities and natural ecosystems. While at a global scale, land-use and land-cover change (LULCC) has emerged as a fundamental indicator for understanding and monitoring both natural and economic processes, it comes with far-reaching implications. These implications surround natural resource management, environmental modelling and assessment, urban and territorial planning, and agricultural production management [1], [2]. As the world's population continues to grow at an unprecedented rate, the demand for food, arable land, and urban space intensifies, placing enormous pressure on finite land resources. Accurate and timely estimation of agricultural production at both local and regional levels has therefore become a scientific and policy imperative; not only to support the growing global population but also to align with international frameworks such as the United Nations' "Zero Hunger" goal under the Sustainable Development Goals (SDGs) [3]-[5].

The consequences of unmanaged land use change are multidimensional and deeply consequential. The conversion of agricultural land to urban or industrial use, deforestation, soil degradation, and the encroachment of settlements into ecologically sensitive zones all contribute to declining food production capacity. It further includes biodiversity loss, and disrupted hydrological cycles. These effects are measurable at both regional and global scales. While major agricultural exporters such as the United States, Brazil, Ukraine, and Kazakhstan are making concerted efforts to scale up production and stabilize prices [6], the situation in developing nations remains structurally precarious. In Nigeria, recent macroeconomic disruptions undermine agricultural productivity [7]. These realities collectively highlight an urgent need for data-driven, spatially explicit tools that can support informed land management and agricultural planning decisions.

Significant efforts have been directed at developing methodologies for detecting and modelling LULCC. Conventional approaches, including post-classification comparison, image differencing, change vector analysis, and principal component analysis, have historically served as the foundation of remote sensing-based change detection [8]. While these tools have contributed meaningfully to the field, they are increasingly strained by the volume, resolution, and heterogeneity of modern geospatial datasets. They rely heavily on manual feature engineering, expert-defined rules, and labour-intensive pre-processing pipelines [2].

The advent of artificial intelligence (AI) using machine learning (ML) has significantly expanded the analytical capacity available for LULCC modelling. ML provide powerful methods for spatial image analysis. It enables the extraction of meaningful patterns from large, high-dimensional datasets that would otherwise be intractable using conventional statistical approaches [2], [5]. Moreover, Deep Learning (DL), in particular, offers transformative potential for LULCC research due to its ability to automatically learn hierarchical, complex features directly from raw data without extensive manual pre-processing [2],[4]. Among DL architectures, Convolutional Neural Networks (CNNs) have demonstrated exceptional performance in spatial feature extraction from satellite imagery. It supports capturing local texture, spectral signatures, and structural patterns across multiple scales [9]. Multimodal DL techniques further extend this capability by integrating heterogeneous data sources, including multispectral satellite imagery, climatic variables, topographic data, and socio-economic indicators [10]. Despite these advances, significant challenges persist in applying DL models to real-world LULCC scenarios, particularly in data-scarce, agrarian communities in developing regions. Existing DL models are predominantly trained and validated on globally curated benchmark datasets, and their transferability to localized contexts, such as the agrarian community, remains limited.

Addressing these limitations, this study proposes a CNN with a Chanel-Wise-Attention mechanism (CNN-CwA) model for LULCC classification and change detection. It is designed specifically to enhance feature discrimination in complex, real-world satellite imagery. The attention mechanism enables the model to dynamically focus on the most informative spatial regions and spectral channels within an image. Consequently, improving sensitivity to subtle land cover transitions that are critical for monitoring agricultural dynamics. The EuroSAT Land Cover Classification dataset is employed to pre-train and validate the proposed model. By combining the spatial feature extraction strengths of CNNs with the selective focus of attention mechanisms, the proposed model aims to overcome the generalization limitations of conventional DL. Aside its methodological contributions, this research provides a replicable framework for LULCC analysis in similar developing-country contexts, supporting evidence-based policymaking toward sustainable land management and food security in Nigeria.

## II. LITERATURE REVIEW

Agricultural productivity, broadly defined as the efficiency with which land, labour, and capital inputs are converted into agricultural output, occupies a central position in global debates. These debates surround food security, economic development, and sustainable resource management [5], [11]. Over the past decades, concerted research efforts spanning technological innovation, policy intervention, and remote sensing science have sought to understand and enhance agricultural output, particularly in regions where farming remains the primary livelihood activity [2], [8]. In Nigeria, agriculture contributed an average of 24% to the nation's GDP

 

between 2013 and 2019 and remains the largest employer of labour, engaging more than 36% of the country's workforce [11]. Despite this structural significance, Nigerian agriculture, particularly in agrarian communities remains undercapitalized, with a tractor density of just 0.27 hp/ha against the FAO-recommended 1.5 hp/ha, reflecting the limited adoption of mechanized and precision farming practices [12]. These realities underscore the urgency of developing more accurate, spatially explicit tools for monitoring land use dynamics and their implications for agricultural productivity.

Technological innovations have progressively transformed approaches to agricultural monitoring and productivity enhancement. The use of Global Positioning System (GPS) technology, Internet of Things (IoT) devices, and remote sensing has advanced precision agriculture, Consequently, farmers are enabled to optimize the application of water, fertilizers, and pesticides, yielding increased outputs while reducing environmental impact [13], [14].

Furthermore, the integration of ML techniques with remote sensing data has opened new analytical frontiers in land cover classification and agricultural productivity assessment. Conventional statistical approaches, while foundational, have proven insufficient for extracting meaningful patterns from the large, high-dimensional datasets generated by modern remote sensing systems. ML algorithms, including Support Vector Machines (SVM), Random Forests (RF), and K-Nearest Neighbour (KNN) classifiers, demonstrated early improvements in land cover mapping accuracy by learning discriminative class boundaries from labelled training samples without relying on explicit spectral thresholds [14], [15]. Wang et al. [2] conducted a comprehensive review of ML algorithms applied to earth observation-based data, concluding RF, CNN, and SVM. The demonstrated competing performance suited for classification and pattern analysis of geospatial data. The authors also observed hybrid approaches consistently demonstrated superior performance in terms of accuracy, efficiency, and computational cost. Also, Generative Adversarial Networks (GANs) applied to simulate urban spatial patterns was observed to performed credibly well.

Samardžić-Petrović et al. [16] investigated SVM for modelling urban land use change across multiple time periods in the Municipality of Zemun, Serbia. The authors observed significant performance improvement when balanced data sampling, informative attribute subsets, and optimally tuned learning parameters were employed on the model. Earlier, Huang et al. [17] proposed an unbalanced SVM framework for modelling urban land use change in Calgary, Canada. Finding shows that the enhanced SVM reliably detected relatively minor land use transitions that standard classifiers typically miss. Shih et al. [18] applied RF classification to multi-date Landsat imagery spanning 1990 to 2015 in Taiwan. They incorporated surface reflectance, Vegetation-Impervious-Soil fractions, and grey-level co-occurrence matrix features to map detailed urban land use change categories. Their findings revealed that overlay-based change mapping outperformed post-classification comparison in accuracy. Upadhyay et al. [19] implemented KNN and Decision Tree classifiers using Python's scikit-learn package to classify LISS-III multispectral satellite imagery of the Mumbai metropolitan region. The land cover classification include forest, water, mangroves, and developed areas. Their work demonstrated the accessibility and utility of lightweight ML approaches for regional LULCC mapping.

## III. METHODOLOGY

The proposed CNN-CwA DL model presents a structured and methodologically rigorous pipeline for LULCC classification. The model comprises four principal stages: data input, pre-processing, deep feature extraction, and classification output. As illustrated in Fig. 1, historical LULC data serve as the primary input, which is subsequently subjected to pre-processing operations, including radiometric correction, normalization, and augmentation. The output of the pre-processing then leads to standardized data splitting. The processed image patches are then passed through a multi-layer CNN backbone. The CNN consists of successive convolutional blocks to extract hierarchical spatial features at increasing levels of abstraction. Consequently, the training progressing from low-level textural and spectral patterns to high-level semantic representations of land cover classes. This encoder pathway mirrors established DL architectures for remote sensing image segmentation, leveraging the proven capacity of CNNs to learn discriminative spatial features across multiple spectral bands without reliance on manual feature engineering [2], [9].

 

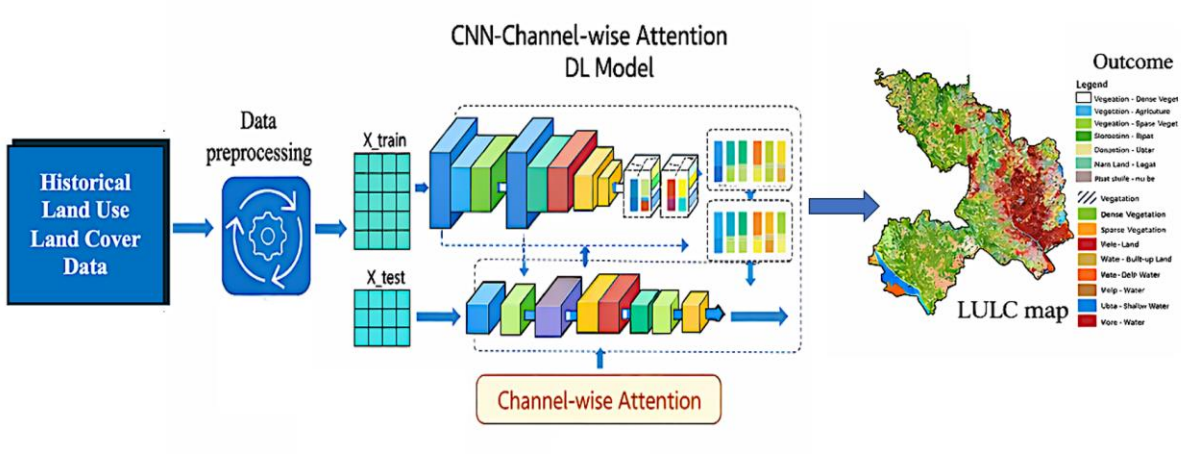


Fig. 1 Conceptual framework for CNN-CwA model

*A. Dataset*

The primary dataset employed in this study is the EuroSAT benchmark dataset. It is a publicly accessible and freely available remote sensing resource derived from Sentinel-2 satellite imagery acquired through the European Space Agency's Copernicus Earth Observation Programme [20]. The dataset encompasses 13 spectral bands spanning the visible, near-infrared, and shortwave infrared portions of the electromagnetic spectrum. It is a rich multi-spectral representation of surface reflectance characteristics for discriminating spectrally similar land cover classes in complex agrarian landscapes. In total, the dataset comprises 27,000 labeled and geo-referenced image patches distributed across 10 distinct land cover classes. The classes include annual crop, permanent crop, forest, herbaceous vegetation, highway, industrial area, pasture, residential area, river, and sea or lake.

*B. Method: Convolutional Neural Network-Channel wise Attention Mode*

Given an input image X ∈ ℝ ^(H×W×C), where H, W, and C denote height, width, and spectral channels respectively, the CNN backbone applies successive convolutional operations to extract hierarchical spatial feature maps. For the l-th convolutional layer, the feature map F(l) is computed as:

$$F^{(l)} = \sigma W^{(l)} * F^{(l-1)} + b^{(l)}$$

where W(l) denotes learnable convolutional filter weights at layer l, b(l) is the bias term, * is convolution, and σ(·) is the ReLU activation function:

$$\sigma x = \max(0, x)$$

The CwA is the defined as, let F ∈ ℝ ^(H′×W′×C′) denote the feature map produced by the CNN encoder. The channel-wise attention mechanism operates in three sequential steps. Spatial dimensions of F are compressed into a channel descriptor vector z ∈ ℝ ^(C′) by GAP:

$$z_c = \frac{1}{H' \times W'} \sum_{i=1}^{H'} \sum_{j=1}^{W'} F_c(i,j), \quad c = 1, 2, \ldots, C'$$

Learned attention weights α are applied via channel-wise multiplication to produce recalibrated feature map. Mitigating vanishing gradients and preserve low-level spatial information, a residual connection is incorporated around each convolutional block. The recalibrated feature map F̂ is then passed through Global Average Pooling to produce a fixed-length feature vector v ∈ ℝ ^(C′), fed into a fully connected classification head:

$$\hat{y} = \text{Softmax}\, W_{fc} \cdot v + b_{fc}$$

The Softmax function produces a probability distribution over N land cover classes:

$$\text{Softmax}\, \hat{y}_n = \frac{e^{\hat{y}_n}}{\sum_{k=1}^{N} e^{\hat{y}_k}}, \quad n = 1, 2, \ldots, N$$

The predicted land cover class ĉ for each image patch is:

$$\hat{c} = \arg\max_n \quad \hat{y}_n$$

*C. Performance Metrics and Vegetation Index*

The evaluation of the proposed CNN-CwA model employs a set of standard performance metrics alongside vegetation-specific indices to assess classification performance and the ecological validity of the predicted land cover maps. Metrics considered is as presented in Tables I and II. Let $TP_n$, $FP_n$, $FN_n$, and $TN_n$ denote the True Positives, False Positives, False Negatives, and True Negatives for class $n$ respectively, where n=1, 2,…,N, where N is the total number of land cover classes.

 

TABLE I
PERFORMANCE METRIC

| **Metric** | **Formula** |
|---|---|
| Intersection over Union IoU (per class) | $\frac{TP_n}{TP_n + FP_n + FN_n}$ |
| Mean (mIoU) | $\frac{1}{N}\sum_{n=1}^{N} IoU_n$ |

TABLE II
COMMON VEGETABLE INDICES

| Index | Formula | Interpretation |
|---|---|---|
| **NDVI** (Normalized Difference Vegetation Index) | `(NIR – Red) / (NIR + Red)` | General vegetation health |
| **GNDVI** (Green NDVI) | `(NIR – Green) / (NIR + Green)` | Chlorophyll content |
| **EVI** (Enhanced Vegetation Index) | `2.5 * (NIR – Red) / (NIR + 6*Red – 7.5*Blue + 1)` | Optimized for high biomass |
| **SAVI** (Soil-Adjusted Vegetation Index) | `(1 + L) * (NIR – Red) / (NIR + Red + L)` (L=0.5) | Minimizes soil brightness effects |

### *D. Experimental Setup*

The experiments were conducted in a controlled computational environment to ensure reproducibility in training and evaluating the proposed CNN-CwA model for LULCC classification. The EuroSAT dataset was preprocessed by resizing all input images to a uniform spatial resolution of 512 × 512 pixels to standardize the input dimensions. Ensuring robust model generalization and mitigate the risk of overfitting inherent in DL models, a k-fold cross-validation strategy was adopted. The model training uses Adam optimizer, learning rate of 0.0001, batch size of 32, and 60 epochs.

Assessing the quality and separability of the learned feature representations produced by the CNN-CwA, t-Distributed Stochastic Neighbour Embedding (t-SNE) was applied to the high-dimensional feature vectors extracted from the penultimate fully connected layer prior to Softmax classification, projecting them into a two-dimensional embedding space for visual inspection [20]. Well-separated and compact clusters in the t-SNE visualization indicate that the model has successfully learned discriminative feature representations for each land cover class, while overlapping clusters reveal potential inter-class confusion, particularly between spectrally similar categories such as cropland and grassland, or sparse vegetation and bare. All experiments were implemented in Python using the TensorFlow and Keras deep learning frameworks, with GPU acceleration employed to manage the computational demands of training the CNN-CwA architecture on the full EuroSAT dataset.

## IV. RESULTS AND DISCUSSION

### *A. Results*

Prior to model training, a preliminary visualisation of the EuroSAT dataset was conducted to examine the distribution of samples across the ten land cover classes. The class distribution reveals a moderately imbalanced dataset, as shown in Fig. 2. The sample counts ranging from a minimum of 2,000 images for the Pasture class to a maximum of 3,595 images for the Sea or Lake class. Three classes, Annual Crop, Forest, and Herbaceous Vegetation, each contribute 3,000 samples, while Highway, Industrial, Permanent Crop, and River classes each contain 2,500 samples, and the Residential class provides 3,000 samples. In addition, the corresponding box plot in Fig. 3 further characterises this distribution, reporting a median of 2,750 samples per class, a minimum of 2,000, a maximum of 3,595, and a positive skewness of 0.17. In all indications, a mild right-skewed distribution with the Sea or Lake class as a slight outlier in sample volume was observed. While the degree of class imbalance is relatively modest compared to many real-world remote sensing datasets, the underrepresentation of the Pasture class is understandable. Being the lowest per-class IoU scores across both models, suggests that sample scarcity contributes meaningfully to classification difficulty. The k-fold cross-validation strategy adopted in this study partially mitigates this imbalance by ensuring that each class is proportionally represented across training and validation splits in every fold iteration.

 

Assessing the quality and discriminability of the feature representations learned by the CNN-CwA, t-SNE was applied to the high-dimensional feature vectors extracted from the penultimate layer of the model across all five cross-validation folds. The resulting two-dimensional embeddings, presented in Fig. 4, reveal consistent clustering behaviour across Fold 1 through Fold 5. The majority of land cover classes are visually separable and geometrically compact clusters in the reduced feature space. Spectrally distinct classes such as Sea or Lake and Forest exhibit particularly tight and well-isolated clusters across all folds, reflecting the model's high confidence in distinguishing these classes. This finding is consistent with their superior per-class IoU scores reported in Table III. In contrast, partial cluster overlap is observed between classes with similar spectral profiles, notably between Annual Crop and Permanent Crop, and between Highway and Industrial Area. Hence, residual inter-class confusion that contributes to the comparatively lower IoU values recorded for these categories.

The models' result is presented in Table III. It shows the per-class IoU scores and computed mIoU values for the baseline CNN and the CNN-CwA model across all ten EuroSAT land cover classes. The CNN-CwA model consistently outperforms the baseline CNN across all ten land cover classes. It achieves a mIoU of 0.8852 compared to 0.8606 for the baseline, representing an overall improvement of +0.0246 (2.86%). The most substantial per-class improvement is observed for the Sea or Lake class, where the CNN-CwA achieves an IoU of 0.9834 against the baseline's 0.9023, a margin of +0.0811. The improvement is attributable to the attention mechanism's capacity to amplify the distinctive spectral signatures of water bodies.

The Pasture class, which recorded the lowest absolute IoU for both models, nonetheless demonstrates the second largest improvement under CNN-CwA of +0.0365. The indication is that channel-wise attention is particularly beneficial for spectrally ambiguous classes. Notable gains are also recorded for River of +0.0292 and Highway of +0.0288. This amount to two structurally narrow and spectrally mixed classes whose fine spatial features are more effectively captured when the model selectively amplifies relevant spectral channels. Vegetation-related classes, including Forest of 0.9001, Herbaceous Vegetation of 0.9134, and Permanent Crop of 0.9011, all surpass the 0.90 IoU threshold under CNN-CwA. Well observed demonstration is that the model reliably discriminates between agronomically significant vegetation categories that are critical for agricultural productivity monitoring area.

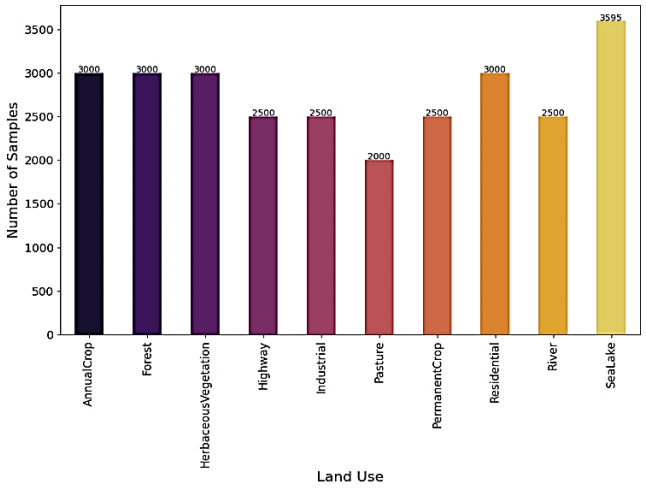


Fig. 2 Bar chart showing the distribution of samples across the ten EuroSAT land cover classes, ranging from 2,000 (Pasture) to 3,595 (Sea or Lake).

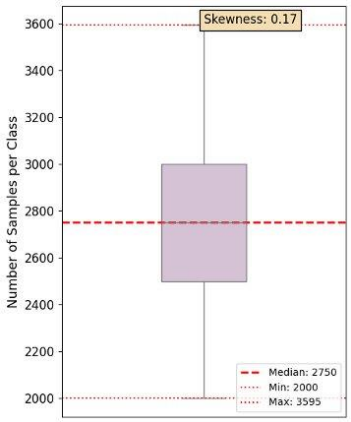


Fig. 3 Sample distribution per class (Median = 2,750; Min = 2,000; Max = 3,595; Skewness = 0.17).

 

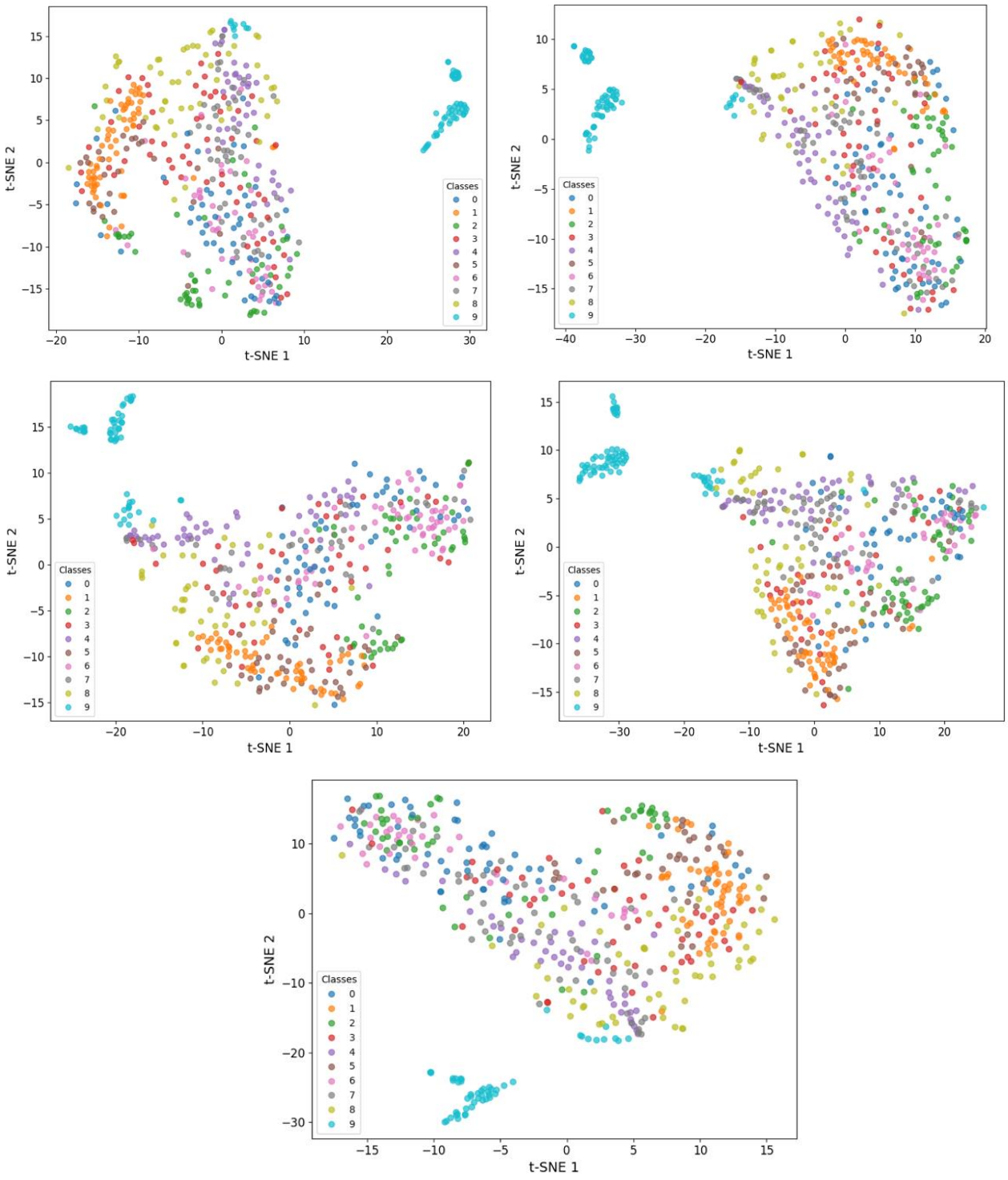


Fig. 4 t-SNE visualisation of learned feature representations across five k-fold cross-validation folds, demonstrating class cluster separability of the CNN-Channel-wise Attention model.

TABLE III
PER-CLASS IOU AND MIOU COMPARISON BETWEEN CNN BASELINE AND CNN-CWA MODEL (HIGHLIGHTED CELLS IN GREEN INDICATE IMPROVEMENTS ≥ 0.03)

| Land Cover Class | CNN IoU | CNN-CwA IoU | Δ Improvement |
|---|---|---|---|
| Annual Crop | 0.8623 | 0.8757 | +0.0134 |
| Permanent Crop | 0.8912 | 0.9011 | +0.0099 |

 

| | | | |
|---|---|---|---|
| Forest | 0.8878 | 0.9001 | +0.0123 |
| Herbaceous Vegetation | 0.9019 | 0.9134 | +0.0115 |
| Highway | 0.8056 | 0.8344 | +0.0288 |
| Industrial Area | 0.8264 | 0.8398 | +0.0134 |
| Pasture | 0.7647 | 0.8012 | +0.0365 |
| Residential Area | 0.9362 | 0.9464 | +0.0102 |
| River | 0.8274 | 0.8566 | +0.0292 |
| Sea or Lake | 0.9023 | 0.9834 | +0.0811 |
| **mIoU** | **0.8606** | **0.8852** | **+0.0246 (+2.86%)** |

Furthermore, the vegetation index results, in Table IV, computed across the five k-fold cross-validation folds reveal consistent and stable patterns in the spectral characterization of the land cover classes within the study area. NDVI values range narrowly from −0.1039 (Fold 0) to −0.1068 (Fold 3), while the GNDVI similarly fluctuates between −0.1499 and −0.1543 across all folds. Also, SAVI values remain tightly clustered between −0.1558 and −0.1602. Consistent negative values are recorded across NDVI, GNDVI, and SAVI in all five folds. It implies non-vegetated or sparsely vegetated surface conditions consistent with the mixed agrarian landscape of local region characterized by bare soil patches, fallow farmland, and peri-urban built-up surfaces (Kussul et al., 2017; Nguyen et al., 2020). In contrast, the EVI records markedly elevated positive values ranging from 15,071.99 (Fold 3) to 18,051.08 (Fold 4). It indicates its sensitivity to atmospheric and canopy background effects. Therefore, there is observed a high inter-fold consistency across all four vegetation indices. While, standard deviations remaining minimal across folds, it confirms that the k-fold partitioning strategy produced well-balanced splits with stable spectral characteristics. In addition, it validates the reliability of the cross-validation framework adopted in this study.

TABLE IV
VEGETABLE INDICES

| Fold | NDVI | GNDVI | EVI | SAVI |
|---|---|---|---|---|
| 0 | -0.10394443 | -0.14992219 | 15611.331 | -0.1558452 |
| 1 | -0.10465597 | -0.15265015 | 17881.102 | -0.1569109 |
| 2 | -0.10520787 | -0.15161838 | 15238.088 | -0.15773867 |
| 3 | -0.106835105 | -0.15427442 | 15071.988 | -0.16017884 |
| 4 | -0.10554487 | -0.15216868 | 18051.084 | -0.15824446 |

### *B. Discussion*

The results demonstrate that the integration of a CwA mechanism into a standard CNN architecture yields consistent and meaningful improvements in LULCC classification accuracy across all land cover classes present in the EuroSAT benchmark dataset. The mIoU improvement of 2.86%, translates into substantively more accurate delineation of agriculturally sensitive land cover boundaries, particularly for spectrally challenging classes such as Pasture, River, and Highway that are directly relevant to land management decision-making in agrarian communities [2].

The t-SNE visualisations corroborate the quantitative findings by confirming that the attention-augmented model learns more discriminative and compact feature representations. It shows a consistent cluster separability maintained across all five cross-validation folds, which implies model stability and generalisability within the training distribution [14]. The mild positive skewness (0.17) in the class distribution and the relatively low sample count for the Pasture class highlight the importance of addressing class imbalance in future iterations. This can be potentially addressed through oversampling strategies or class-weighted loss functions to further improve per-class performance for underrepresented land cover types.

 

Notably, the strong performance of vegetation-related classes, with Forest, Herbaceous Vegetation, and Permanent Crop all exceeding the 0.90 IoU threshold is particularly significant for the agrarian study context. It is helpful in particular where distinguishing between agricultural cropland, natural vegetation, and forest cover is foundational to monitoring changes in agricultural productivity and informing sustainable land use planning decisions [4], [5].

## V. CONCLUSION

This study presented CNN-CwA model for LULCC classification. The proposed model integrates a CwA mechanism into a standard CNN backbone. The CwA enables dynamic recalibration of spectral channel contributions to enhance the discriminative capacity of the network in heterogeneous land cover environments. Trained and validated on the EuroSAT benchmark dataset comprising 27,000 geo-referenced Sentinel-2 satellite image patches across ten land cover classes, the CNN-CwA model demonstrated consistent and measurable improvements. While comparing with the baseline CNN architecture across all evaluation metrics, the model achieved an mIoU of 0.8852, representing a 2.86% improvement over the baseline CNN (mIoU = 0.8606). The most notable per-class gains recorded for Sea or Lake, Pasture, River, and Highway are +0.0811, +0.0365, +0.0292, and +0.0288, respectively. Vegetation-related classes including Forest, Herbaceous Vegetation, and Permanent Crop all surpassed the 0.90 IoU threshold, affirming the model's reliability in discriminating between agronomically significant land cover types that are foundational to agricultural productivity monitoring in communities.

Despite the promising results demonstrated in this study, several limitations warrant acknowledgement. The model was trained exclusively on the EuroSAT dataset which could limits generalization and immediate representation of imagery specifically acquired over the local context region. Additionally, the current study does not incorporate temporal dynamics explicitly into the model architecture, limiting its capacity to capture seasonal vegetation transitions and inter-annual agricultural land use cycles that are central to productivity monitoring in tropical agrarian communities.

Several directions for future research are identified for this study. First, the acquisition and annotation of locally representative multi-temporal satellite imagery of local context and its environs. Second, the incorporation of temporal attention mechanisms, such as Long Short-Term Memory (LSTM) networks or Transformer-based temporal encoders, into the existing CNN-CwA architecture would extend the model's capability to capture land use transition dynamics over time.

## ACKNOWLEDGEMENT

The authors gratefully acknowledge the support and research facilitation provided by the Tertiary Education Trust Fund (TETFund) through its Institution-Based Research Intervention (IBR) scheme and Federal Polytechnic, Ile-Oluji, Ondo State, Nigeria.

# REFERENCES

**[1].** M. F. Baig, M. R. U. Mustafa, I. Baig, H. B. Takaijudin, and M. T. Zeshan, "Assessment of land use land cover changes and future," Water, pp. 1–17, 2022, doi: 10.3390/w14030402.

**[2].** J. Wang, M. Bretz, M. A. A. Dewan, and M. A. Delavar, "Machine learning in modelling land-use and land cover-change (LULCC): Current status, challenges and prospects," Sci. Total Environ., vol. 822, p. 153559, 2022, doi: 10.1016/j.scitotenv.2022.153559.

**[3].** FAO, "Achieving zero hunger," World Food Program, p. 4, 2015.

**[4].** N. Kussul, M. Lavreniuk, S. Skakun, and A. Shelestov, "Deep learning classification of land cover and crop types using remote sensing data," IEEE Geosci. Remote Sens. Lett., vol. 14, no. 5, pp. 778–782, May 2017, doi: 10.1109/LGRS.2017.2681128.

**[5].** N. Zhu, X. Liu, Z. Liu, K. Hu, Y. Wang, J. Tan, M. Huang, Q. Zhu, X. Ji, Y. Jiang, and Y. Guo, "Deep learning for smart agriculture: Concepts, tools, applications, and opportunities," Int. J. Agric. Biol. Eng., vol. 11, no. 4, pp. 21–28, 2018, doi: 10.25165/j.ijabe.20181104.4475.

**[6].** FAO, "World food situation," Food and Agriculture Organization of the United Nations, 2024. [Online]. Available: https://www.fao.org/worldfoodsituation/foodpricesindex/en/

**[7].** ActionAid, "Analysis of the 2024 proposed agriculture budget," ActionAid, Issue Dec. 2023.

**[8].** D. G. Goodin, K. L. Anibas, and M. Bezymennyi, "Mapping land cover and land use from object-based classification: An example from a complex agricultural landscape," Int. J. Remote Sens., vol. 36, no. 18, pp. 4702–4723, 2015, doi: 10.1080/01431161.2015.1088674.

**[9].** C. Zhang, I. Sargent, X. Pan, H. Li, A. Gardiner, J. Hare, and P. M. Atkinson, "Joint deep learning for land cover and land use classification," Remote Sens. Environ., vol. 221, pp. 173–187, 2019, doi: 10.1016/j.rse.2018.11.014.

 

**[10].** J. Yao, B. Zhang, C. Li, D. Hong, and J. Chanussot, "Extended vision transformer (ExViT) for land use and land cover classification: A multimodal deep learning framework," IEEE Trans. Geosci. Remote Sens., vol. 61, pp. 1–15, 2023, doi: 10.1109/TGRS.2023.3284671.

**[11].** T. Oyaniran, "Current state of Nigeria agriculture and agribusiness sector," AfCFTA Workshop, pp. 1–14, Sep. 2020. [Online]. Available: https://www.pwc.com/ng/en/assets/pdf/afcfta-agribusiness-current-state-nigeria-agriculture-sector.pdf

**[12].** T. Economics, "Nigeria food inflation," Trading Economics, 2024. [Online]. Available: https://tradingeconomics.com/nigeria/food-inflation

**[13].** S. Aksoy et al., "Land cover classification methods, Version 1.0," J. Plant Ecol. UK, vol. 3, no. 1, p. 863, 2013, doi: 10.1017/CBO9781107415324.004.

**[14].** S. Talukdar, P. Singha, S. Mahato, Shahfahad, S. Pal, Y.-A. Liou, and A. Rahman, "Land-use land-cover classification by machine learning classifiers for satellite observations — A review," Remote Sens., vol. 12, no. 7, p. 1135, 2020, doi: 10.3390/rs12071135.

**[15].** L. Li, B. Wang, P. Feng, D. Li Liu, Q. He, Y. Zhang, Y. Wang, S. Li, X. Lu, C. Yue, Y. Li, J. He, H. Feng, G. Yang, and Q. Yu, "Developing machine learning models with multi-source environmental data to predict wheat yield in China," Comput. Electron. Agric., vol. 194, p. 106790, Feb. 2022, doi: 10.1016/j.compag.2022.106790.

**[16].** M. Samardžić-Petrović, S. Dragićević, M. Kovačević, and B. Bajat, "Modelling urban land use changes using support vector machines," Trans. GIS, vol. 20, no. 5, pp. 718–734, 2016.

**[17].** B. Huang, C. Xie, R. Tay, and B. Wu, "Land-use-change modelling using unbalanced support-vector machines," Environ. Planning B: Planning Design, vol. 36, no. 3, pp. 398–416, 2009.

**[18].** H. C. Shih, D. A. Stow, K. C. Chang, D. A. Roberts, and K. G. Goulias, "From land cover to land use: Applying random forest classifier to Landsat imagery for urban land-use change mapping," Geocarto Int., vol. 37, no. 19, pp. 5523–5546, 2022.

**[19].** A. Upadhyay, A. Shetty, S. K. Singh, and Z. Siddiqui, "Land use and land cover classification of LISS-III satellite image using KNN and decision tree," in Proc. 3rd Int. Conf. Comput. Sustainable Global Dev. (INDIACom), New Delhi, India, 2016, pp. 1277–1280.

**[20].** P. Helber, B. Bischke, A. Dengel, and D. Borth, "EuroSAT: A novel dataset and deep learning benchmark for land use and land cover classification," IEEE J. Sel. Topics Appl. Earth Observ. Remote Sens., vol. 12, no. 7, pp. 2217–2226, Jul. 2019, doi: 10.1109/JSTARS.2019.2918242.

**[21].** L. Van der Maaten and G. Hinton, "Visualising data using t-SNE," J. Mach. Learn. Res., vol. 9, pp. 2579–2605, 2008.

 